

Real Scalar Field Scattering with Polynomial Approximation around Schwarzschild-de Sitter Black-hole

Molin Liu,^{*} Hongya Liu,[†] Jingfei Zhang, and Fei Yu

School of Physics and Optoelectronic Technology,

Dalian University of Technology, Dalian, 116024, P. R. China

As one of the fitting methods, the polynomial approximation is effective to process sophisticated problem. In this paper, we employ this approach to handle the scattering of scalar field around the Schwarzschild-de Sitter black-hole. The complex relationship between tortoise coordinate and radial coordinate is replaced by the approximate polynomial. The Schrödinger-like equation, the real boundary conditions and the polynomial approximation construct a full Sturm-Liouville type problem. Then this boundary value problem can be solved numerically according to two limiting cases: the first one is the Nariai black-hole whose horizons are close to each other, the second one is when the horizons are widely separated. Compared with previous results (Brevik and Tian), the field near the event horizon and cosmological horizon can have a better description.

PACS numbers: 04.62.+v

Keywords: Hawking radiation, scalar field, polynomial approximation, boundary conditions.

I. INTRODUCTION

In the black-hole physics Hawking radiation[1] is always a very important conception which indicates that black-holes are not perfect black, but radiate thermally and eventually explode. An in-depth discussion of derivation can be obtained in Ref.[2] As for the recent research, one can refer to Ref.[3] Many researchers have developed various methods and techniques to study the black-hole by using the radiating particles, such as the simple Klein-Gordon particles and Dirac particles (for some early works, see Damour and Ruffini[4] and Chandrasekhar[5] respectively). Recently, as for scalar field, Higuchi et al.[6] and Grispino et al.[7] gave its solution outside a Schwarzschild black-hole, Brady et al.[8] studied the Schwarzschild-de Sitter case and Guo et al.[9] made further studies in the Reissner-Nordström-de Sitter one.

The Schwarzschild-de Sitter (SdS) space is a spherically symmetric system.[10] It can be treated as a small Schwarzschild black-hole embedded in de Sitter universe. In this space there are two horizons: one is inner black-hole horizon r_e and the other is outer cosmological horizons r_c . In 2001, Brevik and Simonsen[11] gave a massless scalar field solution by tangent approximation which contains an explicit tangent function. Viewing from the global frame, this method matches r with \tilde{r} very well, where r is the radial coordinate and \tilde{r} is a fitting function. However, its insufficiency is the weak fitting near the two horizons. Even in the intermediate zone, the fitting r with \tilde{r} is not precise enough. In their paper,[11] they have studied for two extreme cases whose horizons are either very close to each other

^{*}Electronic address: mliudl@student.dlut.edu.cn

[†]Electronic address: hylu@dlut.edu.cn

or lie very far away. Afterwards, Tian et al[12] used a polynomial approximation containing 20 monomials and gave another different numerical solution only in the extreme Nariai black-hole. This useful polynomial approximation is more precise than the tangent approximation. Especially, in the leading intermediate zone, the fitting r with a polynomial makes a good match. However, this type of approximation rapidly deteriorates near the horizons, i.e. inappropriate boundary conditions are used. On the other hand, the widely separated horizons case is not considered in Ref.[12] Considering the above situation, we re-study the scattering of a scalar field with polynomial approximation.

This paper is organized as follows: in Section 2, we present the Schwarzschild-de Sitter space and point out the positions of black-hole horizon and cosmological horizon. In Section 3, by the polynomial approximation, the full Sturm-Liouville type problems are solved for two extreme cases. Section 4 is a conclusion. We adopt the signature $(+, -, -, -)$ and put \hbar, c , and G equal to unity. The same setting of field parameters is employed in Ref.[11]

II. SCALAR FIELD IN SCHWARZSCHILD-DE SITTER SPACE

The spherically symmetric metric of the Schwarzschild-de Sitter space[10] is given by

$$ds^2 = f(r)dt^2 - \frac{1}{f(r)}dr^2 - r^2 (d\theta^2 + \sin^2 \theta d\phi^2), \quad (1)$$

where

$$f(r) = 1 - \frac{2M}{r} - \frac{\Lambda}{3}r^2, \quad (2)$$

with the black-hole mass M and the cosmological constant Λ . It is an exact exterior solution of the Einstein field equations for a spherical mass distribution

$$R_{\mu\nu} - \frac{1}{2}g_{\mu\nu}R + \Lambda g_{\mu\nu} = 8\pi GT_{\mu\nu}. \quad (3)$$

Here, we take the cosmological constant Λ as a free parameter. The similar process can be found in Refs.[11, 12, 13] This space is bounded by two horizons — an inner horizon (black-hole horizon) and an outer horizon (cosmological horizon). Under the limit $\Lambda \rightarrow 0$, this metric has exactly the same line-element as the Schwarzschild space. But in the limit of $M \rightarrow 0$, it reduces to the de Sitter one.

Mathematically, expression (2) can be rewritten as

$$f(r) = \frac{\Lambda}{3r}(r - r_e)(r_c - r)(r - r_o). \quad (4)$$

The singularity of metric (1) is determined by $f(r) = 0$. The solutions to this equation are these to inner horizon r_e and outer horizon r_c , as well as a negative solution $r_o = -(r_e + r_c)$. The last one has no physical meaning. Here we only consider the positive solutions. The positions of r_c and r_e are given by

$$\begin{cases} r_c = \frac{2}{\sqrt{\Lambda}} \cos \eta, \\ r_e = \frac{2}{\sqrt{\Lambda}} \cos(120^\circ - \eta), \end{cases} \quad (5)$$

where $\eta = 1/3 \arccos(-3M\sqrt{\Lambda})$ with $30^\circ \leq \eta \leq 60^\circ$. The real physical solutions are accepted only if Λ satisfies $\Lambda M^2 \leq 1/9$. [14] If the cosmological constant Λ reaches its maximum, the Nariai black-hole appears. [15]

A massless scalar field $\Phi(t, r, \theta, \phi)$ is considered here. Using the separable solutions[16]

$$\Phi = \frac{1}{\sqrt{4\pi\omega}} \frac{1}{r} R_\omega(r, t) Y_{lm}(\theta, \phi), \quad (6)$$

the scalar field equation

$$\square\Phi = 0, \quad (7)$$

is decomposed into two differential equations:

$$\begin{aligned} -\frac{1}{f(r)} r^2 \frac{\partial^2}{\partial t^2} \left(\frac{R_\omega}{r} \right) + \frac{\partial}{\partial r} \left(r^2 f(r) \frac{\partial}{\partial r} \left(\frac{R_\omega}{r} \right) \right) \\ - l(l+1) \frac{R_\omega}{r} = 0, \end{aligned} \quad (8)$$

$$\frac{1}{\sin\theta} \frac{\partial}{\partial\theta} \left(\sin\theta \frac{\partial Y_{lm}}{\partial\theta} \right) + \frac{1}{\sin^2\theta} \frac{\partial^2 Y_{lm}}{\partial\phi^2} = -l(l+1) Y_{lm}, \quad (9)$$

where $R_\omega(r, t)$ is the time-dependent radial function and $Y_{lm}(\theta, \phi)$ is the spherical harmonics function. Equation (8) determines the evolution of evaporating black-hole. It is necessary to eliminate the time variable by the Fourier component $e^{-i\omega t}$ via

$$R_\omega(r, t) \rightarrow \Psi_{\omega l}(r) e^{-i\omega t}. \quad (10)$$

So Eq.(8) can be rewritten as

$$\left[-f(r) \frac{d}{dr} \left(f(r) \frac{d}{dr} \right) + V(r) \right] \Psi_{\omega l}(r) = \omega^2 \Psi_{\omega l}(r), \quad (11)$$

whose potential function is given by

$$V(r) = f(r) \left[\frac{1}{r} \frac{df(r)}{dr} + \frac{l(l+1)}{r^2} \right]. \quad (12)$$

Now we introduce the tortoise coordinate

$$x = \frac{1}{2M} \int \frac{dr}{f(r)}. \quad (13)$$

The tortoise coordinate can be expressed by surface gravity as follows:

$$\begin{aligned} x = \frac{1}{2M} \left[\frac{1}{2K_e} \ln \left(\frac{r}{r_e} - 1 \right) - \frac{1}{2K_c} \ln \left(1 - \frac{r}{r_c} \right) \right. \\ \left. + \frac{1}{2K_o} \ln \left(1 - \frac{r}{r_o} \right) \right], \end{aligned} \quad (14)$$

where

$$K_i = \frac{1}{2} \left| \frac{df}{dr} \right|_{r=r_i}. \quad (15)$$

Explicitly, we have

$$K_e = \frac{(r_c - r_e)(r_e - r_o)}{6r_e} \Lambda, \quad (16)$$

$$K_c = \frac{(r_c - r_e)(r_c - r_o)}{6r_c} \Lambda, \quad (17)$$

$$K_o = \frac{(r_o - r_e)(r_c - r_o)}{6r_o} \Lambda. \quad (18)$$

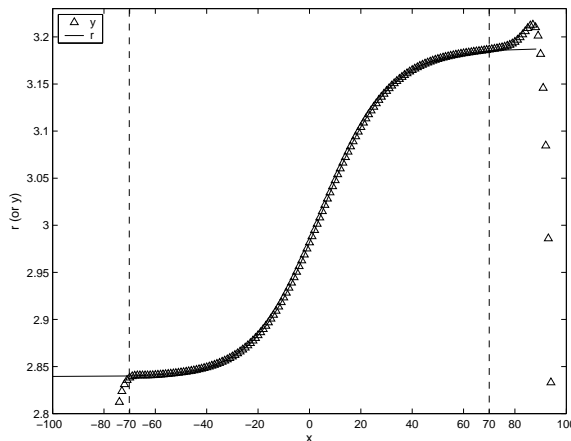


FIG. 1: The radial coordinate r (full line) and polynomial approximation y (triangle-up) versus the tortoise coordinate x with $\Lambda = 0.11$.

By tortoise coordinate transformation (13), the radial equation (11) can be written in the "Regge - Wheeler" form

$$\left[-\frac{d^2}{dx^2} + 4M^2V(r) \right] \Psi_{\omega l}(x) = 4M^2\omega^2\Psi_{\omega l}(x), \quad (19)$$

which has the form of Schrödinger equation of quantum mechanics. It is usually called Schrödinger-like equation. The incoming or outgoing particle flow between inner horizon r_e and outer horizon r_c is reflected and transmitted by the potential barrier $V(r)$. The evolution of wave solution $\Psi_{\omega l}$ of massless scalar field is also determined by potential $V(r)$.

III. FULL STURM-LIOUVILLE TYPE PROBLEM

According to Eqs. (4) and (12), the potential $V(r)$ disappears near black-hole horizon r_e and cosmological horizon r_c . So the potentials near horizons are given as follows:

$$V(r_e) = V(r_c) = 0. \quad (20)$$

Hence near the horizons, Eq.(19) reduces to

$$\left[\frac{d^2}{dx^2} + 4M^2\omega^2 \right] \Psi_{\omega l}(x) = 0. \quad (21)$$

Absolutely, its solutions are $e^{\pm i2M\omega x}$ or their comprehensive form. Taking the real scalar field[11, 12] into account, we choose the real part of its solutions as the boundary condition

$$\Psi_{\omega l} = \cos(2M\omega x). \quad (22)$$

There are two coordinates — radial coordinate r and tortoise coordinate x contained in Eq.(19). However, the source transformation expression (14) is too complicated to invert it to the form of $r = r(x)$. In order to solve Eq.(19) conveniently, it is necessary to use an approximate method for transition

$$r \approx \tilde{r}(x), \quad (23)$$

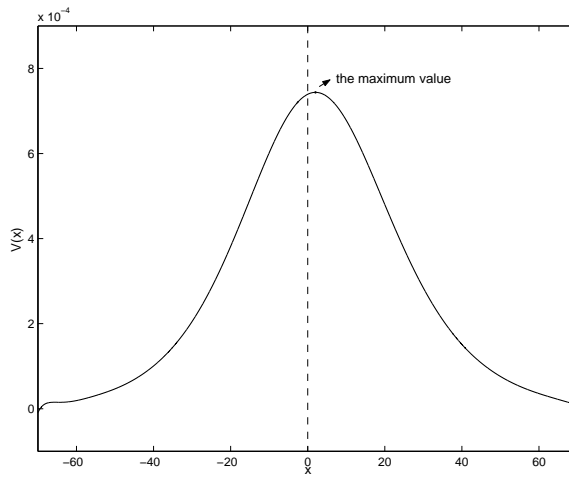


FIG. 2: The potential $V(x)$ versus tortoise coordinate x with $\Lambda = 0.11$, $M = 1$, $l = 1$, where the maximum value is represented by the black point.

where the radial coordinate r is replaced by the fitting function \tilde{r} containing the tortoise coordinate x . Here we use the polynomial approximation[12] to fit r with \tilde{r} . This method involves complicated polynomials unlike the explicit tangent approximation.[11] For any given value of the parameter Λ , we can always find an appropriate approximate method from the above by adjusting the parameters. The difficulty is how to obtain the fitting function (23). Here, we consider the polynomial approximation[12]

$$y = \tilde{r} = \sum_{i=0}^N a_i x^i, \quad (24)$$

where a_i is the coefficient and N is the degree of polynomial. In the various fitting functions, the greatest advantage of the polynomial approximation is that it can obtain the optimal approximation by the adjustable parameter N . One should note that it is wrong to use the bigger N to gain a more accuracy approximation. N must be chosen according to the fitting interval. By combining the potential $V(x)$, the Schrödinger-like equation (19), fitting function (24) with the boundary conditions (26), we can present a full Sturm-Liouville type problem. This kind of boundary value problem is usually used to solve the field equation, such as Refs.[11, 12, 13] Note that the same setting of field parameters as that in Ref.[11] are adopted in the subsections.

A. More Exact Boundary Conditions for Nariai Case: $\Lambda = 0.11$

Nariai solution has been discovered by Nariai,[15] which is the exact solution to the Einstein equation with $\Lambda > 0$ without a Maxwell field. Its topological structure is a (1+1)-dimensional dS spacetime with a round 2-sphere of fixed radius, i.e., $dS_2 \times S^2$. We adopt the same value $\Lambda = 0.11$ as appeared in Refs.[11, 12] Then substituting Λ into Eq.(5), we find the inner horizon is $r_e = 2.8391M$ and the outer horizon is $r_c = 3.1878M$. Just as in Ref.[12], we employ the same polynomial approximation here. The coefficients $\{a_i\}$ are showed in Table 1.

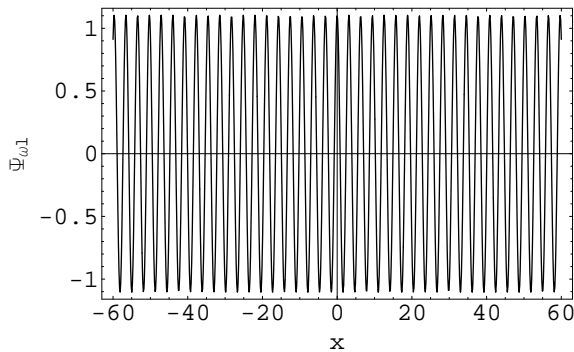


FIG. 3: The wave function $\psi_{\omega l}$ versus the tortoise coordinate x with $\Lambda = 10^{-3}$, $M = 1$ and $l = 1$.

TABLE I: The coefficients of degree 20 polynomial with $\Lambda = 0.11$.

$a_0 = 2.9817$	$a_1 = 6.5107 \times 10^{-3}$	$a_2 = 4.0912 \times 10^{-5}$
$a_3 = -2.9913 \times 10^{-6}$	$a_4 = -3.4895 \times 10^{-8}$	$a_5 = 1.6009 \times 10^{-9}$
$a_6 = 2.3413 \times 10^{-11}$	$a_7 = -8.0083 \times 10^{-13}$	$a_8 = -1.1964 \times 10^{-14}$
$a_9 = 3.3845 \times 10^{-16}$	$a_{10} = 4.3110 \times 10^{-18}$	$a_{11} = -1.0899 \times 10^{-19}$
$a_{12} = -1.0120 \times 10^{-21}$	$a_{13} = 2.4364 \times 10^{-23}$	$a_{14} = 1.4031 \times 10^{-25}$
$a_{15} = -3.4329 \times 10^{-27}$	$a_{16} = -9.5242 \times 10^{-30}$	$a_{17} = 2.6439 \times 10^{-31}$
$a_{18} = 1.5652 \times 10^{-34}$	$a_{19} = -8.0402 \times 10^{-36}$	$a_{20} = 4.3262 \times 10^{-39}$

The boundary conditions in Ref.[12] came directly from the original work in Ref.[11],

$$\Psi_{\omega l}(x)|_{x=-100} = \Psi_{\omega l}(x)|_{x=100} = \cos(200M\omega). \quad (25)$$

However, it is not appropriate to use Eq.(25) directly as the boundary conditions do not consider the new approximation. The intervals of the boundary conditions should be in accord with the fitting intervals. Now, we present the inappropriate boundary conditions in previous polynomial approximation.[12] One can treat the polynomial (24) as a function varying with x for $N = 20$. The coefficients are listed in Table.1. The functional images of Eqs.(24) and (14) both are drawn in Fig.1. It is shown that \tilde{r} (or y) and r match exactly in the intermediate zone. However, near the horizons r_e and r_c , the polynomial behavior takes over and the approximation quickly deteriorates. Especially, there are significant differences between r and y in the two intervals, $[-70, -100]$ and $[70, 100]$, along the horizontal axis. Because of the unnecessary intervals, the singular peak has arisen in the waves (one can refer to Figs.4 and 5 in Ref.[12]). This problem can be solved by reducing the interval x from $[-100, 100]$ to $[-70, 70]$. Hence, the effective interval in the radial direction has been changed from $[2.8391M, 3, 1878M]$ to $[2.8382M, 3.1865M]$. After removing the useless intervals: $[-70, -100]$ and $[70, 100]$, we obtain another exact boundary conditions

$$\Psi_{\omega l}(x)|_{x=-70} = \Psi_{\omega l}(x)|_{x=70} = \cos(140M\omega). \quad (26)$$

The potential $V(x)$ of Nariai black-hole is plotted in the range of $-70 \leq x \leq 70$ in Fig.2, with maximum value $V = 7.4381 \times 10^{-4}$ corresponding to $x = 2.0352$. By using Mathematica software in book,[17] one can solve it numerically as a boundary value problem, where the command NDSolve is used. The amplitude versus the tortoise

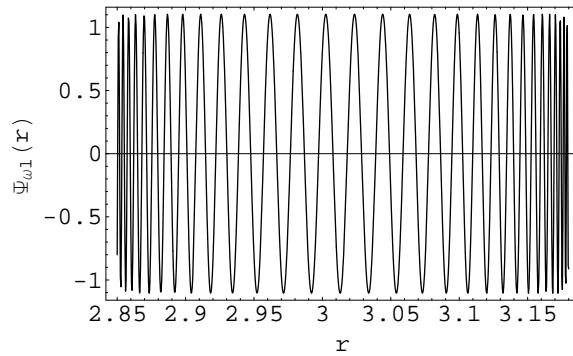


FIG. 4: The variation of the wave function $\psi_{\omega l}$ with the radial coordinate r for $\Lambda = 10^{-3}$, $M = 1$ and $l = 1$.

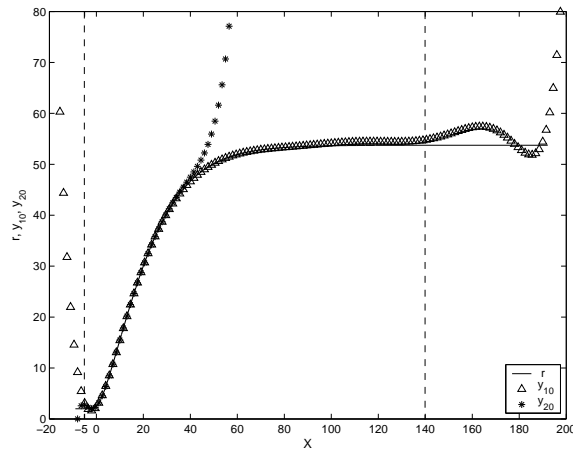


FIG. 5: The radial coordinate r (full line), the 10-th polynomial y_{10} (triangle-up) and the 20-th polynomial y_{20} (star) versus the tortoise coordinate x with $\Lambda = 10^{-3}$.

coordinate is shown in Fig.3. It is seen that the solution $\Psi_{\omega l}(x)$ is similar to a harmonic wave without considering the decay factor $1/r$ in the ansatz (6). The radial equation (8) is transformed into a standard wave equation by useful tortoise transformation (13). With the real boundary conditions (cosine functions), the harmonic wave arises naturally. Taking into account the actual case, we also plot the amplitude versus r in Fig.4. This diagram illustrates clearly that waves stack up near r_e and r_c .

For the case of Brevik's work, because the tangent approximation does not work well near the two horizons (see Fig.3 in Ref.[11]), waves do not pile up near the outer horizon r_c (see Fig.6 in Ref.[11]). For the case of Tian's work, there is a singular peak in waves near $x = 2.8582$ (or $r \sim 3$) (see Figs.4 and 5 in Ref.[12]). The occurrence of this singular peak is due to inappropriate boundary conditions (25) chosen. In this paper, the precise polynomial approximation is kept, but the boundary conditions (25) are replaced by the new exact ones (26). However, viewing from the numerical solutions shown in Figs.3 and 4, we can say that the afore-mentioned deficiencies have been remedied.

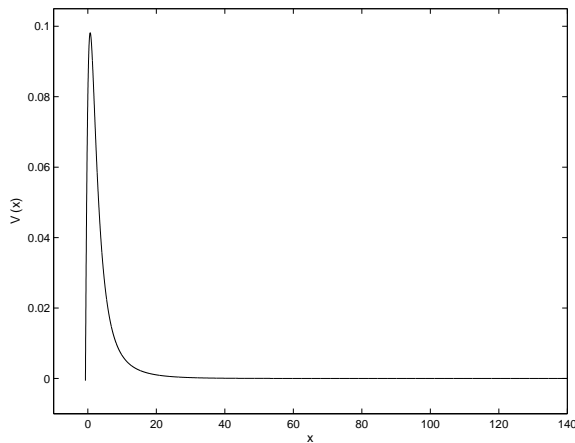


FIG. 6: The potential $V(x)$ versus tortoise coordinate x with $\Lambda = 10^{-3}$, $M = 1$, $l = 1$.

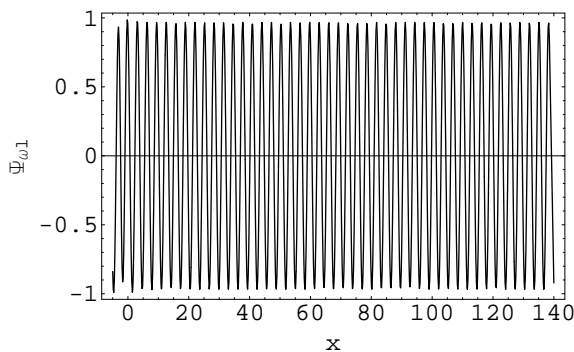


FIG. 7: The variation of the wave function $\psi_{\omega l}$ with the tortoise coordinate x for $\Lambda = 10^{-3}$, $M = 1$ and $l = 1$.

B. Widely Separated Horizons Case: $\Lambda = 0.001$

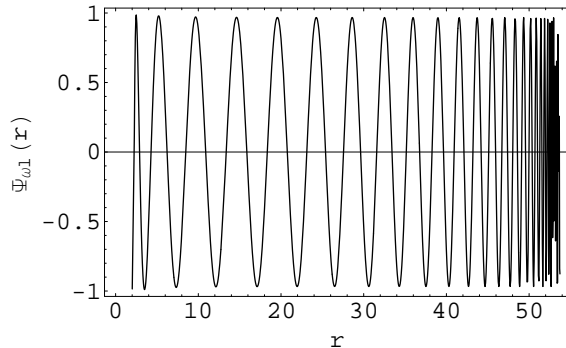
The accelerating universe phenomenon can be easily explained by a repulsive force produced by non-zero and positive cosmological constant $\Lambda_0 \sim 10^{-52} m^{-2}$. [18] The cosmological constant has very interesting gravitational effects on various astrophysical scales such as the gravitational lensing statistics of extragalactic surveys, [19] large-scale velocity flows, [20] the effects on observation in small system (Galactic, [21] Planetary, [22] and Solar [23]). Considering the widely separated horizons case, we take the cosmological constant $\Lambda = 10^{-3}$, which is employed as a general setting in many works. [11, 13] Of course, the other value of cosmological constant subjected to the condition $\Lambda M^2 \leq 1/9$ also can be adopted in principle. Here we take the same value as that in Ref. [11]

In the polynomial approximation, the number of terms can be selected at random in principle. Two points determine one line or an approximating polynomial of degree 1; three points determine an approximating polynomial of degree 2, and so on; while $n + 1$ points determine the approximating polynomial of degree n . However, the polynomial with higher degree presents some defective numerical characteristics. With increasing degree, the fitting curve becomes lack of smoothness because the higher degree polynomial can be differentiated many times before it reduces to zero. We thus choose a right polynomial rather than a higher degree one.

The polynomials with 20-th degree (y_{20}) and 10-th degree (y_{10}) are plotted in Fig.5. We can read that the fitting

TABLE II: The coefficients in the approximating polynomial of degree 10

$a_0 = 2.3895$	$a_1 = 0.64096$	$a_2 = 0.11802$
$a_3 = -6.7621 \times 10^{-3}$	$a_4 = 1.8818 \times 10^{-4}$	$a_5 = -3.2408 \times 10^{-6}$
$a_6 = 3.6365 \times 10^{-8}$	$a_7 = -2.6487 \times 10^{-10}$	$a_8 = 1.2019 \times 10^{-12}$
$a_9 = -3.0754 \times 10^{-15}$	$a_{10} = 3.3792 \times 10^{-18}$	

FIG. 8: The variation of the wave function $\psi_{\omega l}$ with the radial coordinate r for $\Lambda = 10^{-3}$, $M = 1$ and $l = 1$.

interval of y_{10} is $[-5, 140]$ and the fitting interval of y_{20} is $[-5, 40]$. Obviously, the former is much wider than the latter. Here, we adopt the 10-th degree polynomial as fitting function (24). The coefficients are listed in Table 2. Using this approximation, the potential $V(x)$ is plotted in Fig.6. The curve peak approaches the event horizon r_e and is far apart from the cosmological horizon r_c . Like the former case, this kind of boundary value problem can be solved numerically[17] with a more general setting which is more faithfully representing our world. The numerical solutions $\Psi_{\omega l}(x)$ and $\Psi_{\omega l}(r)$ are shown in Figs.7 and 8, respectively. Obviously, with decreasing Λ the waves become much sparser near r_e and much denser near r_c . Otherwise, since all parts of the potential are in the region of $x > 0$, the wave solutions $\Psi(x)$ and $\Psi(r)$ are concentrated in the positive horizontal axis too.

IV. CONCLUSION

We have solved the real scalar field numerically with the polynomial approximation. Unlike the previous original work,[12] we have not only surveyed a more general setting of field parameters, i.e. the widely separated horizons case, but also selected more precise boundary conditions. We summarize what have been achieved as follows.

1 Polynomial approximation is an important and comprehensible approximate method. In this paper this method has been used to fit the radial coordinate with the tortoise coordinate. Unlike the tangent approximation,[11] one main merit of this method is that there is an adjustable parameter, the degree of the polynomial. The degree of the polynomial must be selected to ensure that we can obtain the maximum fitting interval. From the analysis in this paper, we find that the degree of the polynomial should be reduced with increasing cosmological constant. When we consider two extreme cases with $\Lambda = 0.11$ and $\Lambda = 0.001$, the degree should be reduced from 20 to 10.

2 As for the Nariai black-hole, because the potential barrier $V(r)$ (12) vanishes near the two horizons, Eq.(22) becomes a universal boundary condition for real solution case. But the different fitting intervals need different

boundary conditions. So it has to choose a well and suitable one according to the quality of fitting. In this paper, we have chosen another exact boundary condition. Although the previous polynomial approximation is more accurate to match r with \tilde{r} in the intermediate zone, the interval of x does not keep the original one $([-100, 100])$. It is illustrated clearly in Fig.1. Obviously, when the tortoise coordinate x is in the range of $[-100, -70]$ or $[70, 100]$, the approximation (24) quickly deteriorates. So it is necessary to use the new interval $[-70, 70]$ to replace the previous one $[-100, 100]$. As mentioned in the above sections, by tortoise coordinate transformation the radial equation can be rewritten as a standard wave equation form. By combining with the real boundary condition (cosine function form), the harmonic wave appears. Otherwise, for the compactness of the tortoise coordinate the waves pile up near the horizons naturally. These effects in the Nariai case in the Brevik's work[11] are subtle and subclinical near the cosmological horizon r_c . After rebuilding the scalar field in this paper, we find that there is no singular peak in waves, and the waves pile up near the two horizons r_e and r_c , which refreshes previous works in Refs.[11, 12]

3 For the widely separated horizons case, the dimensional version of $\Lambda = 10^{-3}$ reads

$$\Lambda \left(\frac{GM}{c^2} \right) = 10^{-3}, \quad (27)$$

where G is the gravitational constant, c is the speed of light and M is the mass of black-hole. Considering a usual Stellar Black Hole, we assume the mass M equal to ten sun masses (i.e. $M = 10M_\odot$). It is known that for the Solar system we have

$$\frac{GM_\odot}{c^2} = 1.475km. \quad (28)$$

Substituting the mass M and the notation (28) into Eq.(27), we can obtain a dimensional cosmological constant

$$\Lambda = 4.6 \times 10^{-16} cm^{-2}. \quad (29)$$

Using the same method, we can also obtain the dimensional cosmological constant in the Nariai case.

$$\Lambda = 2.4 \times 10^{-13} cm^{-2} \quad (30)$$

Although the values are much larger than the observed value Λ_0 , it is very necessary to further research them. After all, the space could be a Schwarzschild one if we take the observational value $10^{-52}m^{-2}$.

V. ACKNOWLEDGE

Project supported by the National Basic Research Program of China (Grant No. 2003CB716300) and National Natural Science Foundation of China (Grant No. 10573003).

[1] Hawking S W 1974 *Nature* 248 30

Hawking S W 1975 *Commun. Math. Phys.* 43 199

[2] Brout R, Massar S, Parentani R and Spindel P 1995 *Phys. Rept.* 260 329

[3] Wu S Q and Cai X 2002 *Chin. Phys.* 11 661

Jiang Q Q, Yang S Z and Wu S Q 2006 *Chin. Phys.* 15 2523

- Ren J, Cao J L and Zhao Z 2006 *Chin. Phys.* 15 2256
- Hu Y P, Zhang J Y and Zhao Z 2007 *Acta Phys. Sin.* 56 683 (in Chinese)
- Jiang Q Q and Wu S Q 2006 *Acta Phys. Sin.* 55 4428 (in Chinese)
- Cao J L 2006 *Acta Phys. Sin.* 55 2682 (in Chinese)
- [4] Damour T and Ruffini R 1976 *Phys. Rev. D* 14 332
- [5] Chandrasekhar S 1976 *Proc. Royl. Soc. Lond.A* 349 571
- [6] Higuchi A, Matsas G E A and Sudarsky D 1998 *Phys. Rev. D* 58 104021 gr-qc/9806093
- [7] Crispino L C B, Higuchi A and Matsas G E A 2000 *Class. Quant. Grav.* 17 19 gr-qc/9901006
- [8] Brady P R, Chambers C M, Laarakkers W G and Poisson E 1999 *Phys. Rev. D* 60 064003 gr-qc/9902010
- [9] Guo G H, Gui Y X and Tian J X 2003 *Int. J. Mod. Phys. A.* 18 4829
- [10] Rindler W 2001 *Relativity* (Oxford: Oxford University Press)
- [11] Brevik I and Simonsen B 2001 *Gen. Rel. Grav.* 33 1839
- [12] Tian J X, Gui Y X and Guo G H 2003 *Gen. Rel. Grav.* 35 1473 gr-qc/0304009
- [13] Liu M L, Liu H Y, Xu L X and Wesson P S 2006 *Mod. Phys. Lett. A* 21 2937 gr-qc/0611137
- Kanti P, Grain J and Barrau A 2005 *Phys. Rev. D* 71 104002 hep-th/0501148
- Liu M L, Liu H Y, Luo F and Xu L X 2007 *Gen. Rel. Grav.* 39 1389 gr-qc/0705.2465
- [14] Liu H Y 1991 *Gen. Rel. Grav.* 23 759
- [15] H Nariai 1950 *Sci. Rep. Tohoku Univ.* 34 160
- H Nariai 1951 *Sci. Rep. Tohoku Univ.* 35 62
- Liu M L, Liu H Y, Wang C X and Ping Y L 2007 *Int. J. Mod. Phys. A* 22 4451 gr-qc/0707.0520
- [16] Jensen B P, Candelas P 1986 *Phys. Rev. D* 33 1590
- [17] Wolfram S 1996 *The Mathematica Book 3rd ed* (Cambridge: Wolfram Media/Cambridge Univ. Press)
- [18] Schmidt B P et al. [Hi-Z Supernova Team Collaboration] 1998 *Astrophys. Journ.* 507 46 astro-ph/9805200
- Riess A G et al. 1998 *Astron. J.* 116 1009 astro-ph/9805200
- Peebles P J E and Ratra B 2003 *Rev. Mod. Phys.* 75 559 astr-ph/0207347v2
- Ostriker J P and Steinhardt P T 1995 *Nature* 377 600
- [19] Quast R and Helbig P 1999 *Astron. Astrophys.* 344 721 astro-ph/9904174
- [20] Zehavi I and Dekel A 1999 *Nature* 401 252 astro-ph/9904221
- [21] Whitehouse S B and Kraniotis G V 1999 astro-ph/9911485
- [22] Cardona J and Tejeiro J 1998 *Ap. J.* 493 52
- [23] Kagramanova V, Kunz J and Lämmerzahl C 2006 *Phys. Lett. B* 634 465 gr-qc/0602002v2